European Journal of Radiology 134 (2021) 109412

Contents lists available at ScienceDirect

European Journal of Radiology

journal homepage: www.elsevier.com/locate/ejrad

Comparison between 3-point Dixon- and CHESS-based OMERACT-recommended MRI protocols in hands of patients with suspicion of early rheumatoid arthritis

Thomas Kirchgesner [a,*,1], Maria Stoenoiu [b,1], Nicolas Michoux [a], Patrick Durez [b], Bruno Vande Berg [a]

[a] Department of Medical Imaging, Musculoskeletal Imaging Unit, Cliniques universitaires Saint-Luc, Université Catholique de Louvain, Institut de Recherche Expérimentale et Clinique (IREC), Avenue Hippocrate 10 1200, Brussels, Belgium
[b] Department of Rheumatology, Cliniques universitaires Saint-Luc, Université Catholique de Louvain, Institut de Recherche Expérimentale et Clinique (IREC), Avenue Hippocrate 10 1200, Brussels, Belgium

ARTICLE INFO

Keywords:
MRI
Dixon
CHESS
Rheumatoid arthritis
Fat
Hand

ABSTRACT

Purpose: To compare fat suppression effectiveness, image quality and disease activity scores between MRI protocols based on the Dixon method and the Chemical Shift Selective (CHESS) technique in hands of patients with suspicion of early rheumatoid arthritis (RA).
Method: Both hands of 28 patients (19 women; mean age 45.2 years old) with suspicion of early RA were prospectively imaged with Dixon- and CHESS-based OMERACT recommended protocols at 1.5 T including fat-suppressed T2-weighted and contrast-enhanced T1-weighted imaging. Two radiologists (R1/R2) separately assessed effectiveness of fat suppression and determined RAMRIS scores woth the Dixon- and CHESS-based protocols. R1 repeated the RAMRIS scoring and measured contrast-to-noise ratios (CNRs) on Dixon and CHESS images. Statistics included 2-way ANOVA test for the comparison of CNRs and Bland-Altman methodology for inter-technique and intra-observer agreement ($p < 0.05$).
Results: Fat suppression failure occurred in up to 1 patient with the Dixon- and 25 patients with the CHESS-based protocols. CNRs were significantly higher on T1-weighted and lower on T2-weighted Dixon images than on the corresponding CHESS images ($p \leq 0.042$). Median bias of the difference between Dixon- and CHESS-based RAMRIS scores was not significantly different from 0 (−0.8 to +1.0 and −1.1 to +1.4 for R1/R2). Median bias of the difference between RAMRIS scores at first and second readings was significantly different from 0 with the CHESS-based protocols (−0.8 to +1.7) but not with the Dixon-based protocols (+0.0 to +1.0).
Conclusions: Dixon sequences yield more effective fat suppression and more reproducible RAMRIS scoring than CHESS sequences in hands with suspicion of early RA.

1. Introduction

Magnetic resonance imaging (MRI) is more sensitive than clinical examination and radiographs to detect early inflammatory changes (synovitis, tenosynovitis, osteitis) and structural damage (bone erosions) in patients with rheumatoid arthritis (RA) [1].

Outcome Measures in Rheumatology (OMERACT), a multi-institution study group, developed a scoring system to assess RA activity at MRI, the Rheumatoid Arthritis MRI scoring system (RAMRIS) [2,3]. OMERACT recommends the following MRI protocol to perform RAMRIS: i. T1-weighted images to assess erosions; ii. fat-saturated T2-weighted or STIR images to assess osteitis; iii. T1-weighted images after intravenous contrast material injection to assess synovitis and tenosynovitis.

Fat signal suppression including on contrast-enhanced T1-weighted imaging is useful to image RA as it allows higher sensitivity for lesion

Abbreviations: CHESS, Chemical Shift Selective; CNR, contrast-to-noise ratio; GRE, gradient echo; OMERACT, Outcome Measures in Rheumatology; RA, rheumatoid arthritis; RAMRIS, Rheumatoid Arthritis MRI scoring system; SE, spin echo.

* Corresponding author.
E-mail address: thomas.kirchgesner@uclouvain.be (T. Kirchgesner).

[1] Thomas Kirchgesner and Maria Stoenoiu equally contributed to this work.

https://doi.org/10.1016/j.ejrad.2020.109412
Received 28 July 2020; Received in revised form 31 August 2020; Accepted 9 November 2020
Available online 12 November 2020
0720-048X/

detection [4–6]. The Chemical Shift Selective (CHESS) technique has been used to obtain fat signal suppression at hand MRI during the past decades [6–9]. Recently the Dixon method emerged in clinical practice and gained particular interest in musculoskeletal imaging [10].

Previous studies compared fat suppression effectiveness and image quality between Dixon and CHESS sequences in hands of healthy volunteers [11–13]. To our knowledge, no previous study compared complete Dixon- and CHESS-based OMERACT recommended MRI protocols for the quantification of synovitis, tenosynovitis, osteitis and erosions according to RAMRIS in hands of patients with suspected RA [11].

The aim of our study was to compare Dixon- and CHESS-based OMERACT-recommended MRI protocols for the effectiveness of fat suppression, the image quality and the RAMRIS scoring in hands of patients with suspicion of early RA.

2. Material and methods

2.1. Patients

Study participants were recruited by two senior rheumatologists among new outpatients of our Department of Rheumatology between January 2016 and December 2017. Inclusion criteria were: i. age older than 18 years old; ii. suspicion of active rheumatoid arthritis at hands by a senior rheumatologist based on clinical and biological data; iii. active disease for less than 24 months; iv. no history of treatment by disease-modifying anti-rheumatic drugs (DMARDs); v. no contraindication to MRI; vi. signed agreement to participate to the study. Clinical evaluation with tender and swollen joints count, CRP (C-reactive protein) blood level and calculation of disease activity score 28 (DAS28-CRP) were obtained for all study participants.

This prospective study was performed with Institutional Review Board approval and after the obtention of written informed consent from each study participant.

2.2. MR imaging

MRI examinations were performed on a 1.5 T MR scanner (Optima MR450w; General Electric, United States of America) with a flexible 16-channel medium-sized extremity coil (Flex coil; General Electric, United States of America). Study participants were positioned in prone procubitus with arms extended above head and hands joined palm-to-palm. Hands were separated by a 4-millimeter-thick plastic plate and maintained with straps. A vitamin E capsule was placed on the dorsal aspect of the right wrist. The flexible coil was placed around the hands and maintained with straps.

Both hands of each study participant were simultaneously imaged with the OMERACT-recommended sequences using the 3-point Dixon method ("Dixon-based protocol") and the CHESS technique ("CHESS-based protocol"). Dixon-based protocol included T1-weighted "IDEAL" Dixon sequence(s) without contrast material injection, T2-weighted "IDEAL" Dixon sequence and contrast-enhanced T1-weighted "IDEAL" Dixon sequence(s). CHESS-based protocol included T1-weighted sequence(s) without contrast material injection, T2-weighted CHESS sequence and contrast-enhanced T1-weighted CHESS sequence(s). One out of two study participants was imaged with 2D spin echo (SE) T1-weighted sequences in the axial and coronal planes before and after intra-venous Gadolinium contrast-material injection ("2D SE T1" group) while the other one was imaged with axial 3D fast spoiled gradient echo (GRE) T1-weighted sequences ("3D GRE T1" group) in accordance with the OMERACT recommendations [3].

All study participants were injected with 2 ml/kg of gadoterate meglumine (Dotarem®; Guerbet, France). The acquisition order of the contrast-enhanced sequences (Dixon or CHESS sequences first) was alternated among study participants. All T2-weighted sequences were obtained in the coronal plane. MRI sequences parameters are summarized in Table 1. Investigated area extended from distal radio-ulnar joints to metacarpophalangeal joints of both hands. Acquisition durations were 15 min 57 s and 16 min 01 s with the Dixon-based protocols of the "2D SE T1" and "3D GRE T1" groups respectively and 8 min 39 s and 6 min 57 s for the CHESS-based protocols of the "2D SE T1" and "3D GRE T1" groups respectively. Patients with incomplete MRI examination according to the study requirements or MRI examination not meeting quality standards were excluded from the study.

In May 2019, a data manager created sets of images including one Dixon- and one CHESS-based set for each of the study participants. The Dixon-based sets contained T1-weighted Dixon in-phase images without contrast material injection, T2-weighted Dixon water-only images and contrast-enhanced T1-weighted Dixon water-only images. The CHESS-based sets contained standard T1-weighted images without contrast material injection, T2-weighted CHESS images and contrast-enhanced T1-weighted CHESS images. After deletion of study participant and fat suppression information, the Dixon and CHESS-based sets were numerically labelled in a random order and archived in our research picture archiving communication system (Carestream Vue 12.1.6.1005; Carestream Health, Inc., Canada). No image was lost at archiving.

2.3. MR imaging analysis

Between June and August 2019, two radiologists with four years (R1) and 30 years (R2) of experience in musculoskeletal imaging and

Table 1
Parameters of the sequences of the study protocol.

	Axial 2D SE T1 Dixon	Coronal 2D SE T1 Dixon	Axial 3D GRE T1 Dixon	Coronal 2D SE T2 Dixon	Axial 2D SE T1 (CHESS)	Coronal 2D SE T1 (CHESS)	Axial 3D GRE T1 (CHESS)	Coronal 2D SE T2 CHESS
Field of view (cm)	16.8–24	16.8–24	16–20	16.8–24	16.8–24	16.8–24	16–20	16.8–24
Slice thickness (mm)	2.5	2.5	1.6	2.5	2.5	2.5	1.6	2.5
Spacing (mm)	0.3	0.3	/	0.3	0.3	0.3	/	0.3
Repetition time (ms)	442–741	618–623	10.9–11.2	5524–5851	427–661 (530–734)	535–550 (725–734)	6.8–6.9 (16.4–16.5)	5834–5909
Effective echo time (ms)	11.6	11.6	5.96	68.6	10.1	10.1	4.2	66.2
Flip angle (°)	160	160	12	160	160	160	12	160
Echo train length	3	3	/	11	3	3	/	11
Acquisition matrix	288 × 224	288 × 224	256 × 256	288 × 256	512 × 288	512 × 288	256 × 256	288 × 224
Reconstruction matrix	512 × 512	512 × 512	512 × 512	512 × 512	512 × 512	512 × 512	512 × 512	512 × 512
NEX	1	1	1	1	1	1	1	2
Bandwidth (kHz)	62.5	62.5	50	83.3	41.7	41.7	50	27.8
Number of slices	44–48	42	192	42	44–48	42	192	42
Duration	3 min 08s	2 min 59s	6min 09s	3 min 43s	1 min 11 s (1 min 56 s)	1 min 09s (1 min 56 s)	1 min 19s (3 min 11 s)	2 min 27s

previous experience in RAMRIS scoring [14] separately analyzed all the sets to evaluate fat suppression effectiveness and to score disease activity. Between September and October 2019, R1 repeated the RAMRIS scoring of all the sets of images to evaluate intra-observer agreement.

Fat suppression effectiveness was assessed on fat-suppressed images in the areas to score according to the RAMRIS scoring system. Fat suppression was considered effective when diffuse homogeneous low signal intensity was present in epiphyseal bone marrow or adjacent fat on all slices through the joint and completely failed when diffuse high signal intensity in epiphyseal bone marrow or periarticular fat was present on all slices through the joint. Fat suppression was considered partially failed when it was neither effective nor completely failed.

Disease activity was scored according to OMERACT recommendations [3]. Synovitis was scored from 0 (absence of synovitis) to 3 (severe synovitis) in 8 joints per hand (distal radioulnar joint, radiocarpal joint, intercarpal and carpometacarpal joints and each metacarpophalangeal joint), tenosynovitis from 0 (absence of tenosynovitis) to 3 (severe tenosynovitis) in 13 tendons per hand (6 extensor tendon compartments and 3 flexor tendon compartments at the wrist and the flexor tendons at the level of each metacarpophalangeal joint), osteitis from 0 (no osteitis) to 3 (severe osteitis) and erosions from 0 (no erosion) to 10 (complete destruction) in 23 bones per hand (distal radius, distal ulna, carpal bones, metacarpal bases, metacarpal heads and proximal phalangeal bases) [3]. Readers used T1-weighted images to score erosions, fat-suppressed T2-weighted images to score osteitis and contrast-enhanced fat-suppressed T1-weighted images to score synovitis and tenosynovitis [15]. In case of fat suppression failure on T2-weighted images, readers were allowed to use other sequences to assess osteitis. If scoring of a joint, tendon or bone was not feasible, it was declared "non assessable".

In November 2019, R1 measured contrast-to-noise ratio (CNR) in fat-suppressed images with a dedicated software (Osirix 10.0; Pixmeo SARL, Switzerland) [16].

Quantitative measurements of signal intensity (SI) were performed on axial contrast-enhanced fat-suppressed T1-weighted images for defined regions of interest (ROIs) between 3 and 25 mm^2 (mean 13.6 mm^2) in size in the enhanced synovial tissue of joints scored 3 according to RAMRIS by at least one reader whatever the MRI protocol. Axial contrast-enhanced T1-weighted Dixon water-only and axial contrast-enhanced T1-weighted CHESS images of the same patient were synchronized. First, an ellipse-shaped ROI was placed in the area with the highest SI of the targeted synovium on the CHESS image. Care was taken that ROIs did not include interdigital vessels. On the same image, another ROI identical to the first ROI was placed in normal homogeneous muscle tissue and an ellipse-shaped ROI larger than 40 cm^2 was placed in an artifact-free zone of the air around the hands. Defined ROIs were automatically propagated into the corresponding Dixon image. CNR was calculated with the following formula: $CNR^{synovitis} = 0.66 \times (SI^{synovitis}\text{-}SI^{muscle})/SD^{air}$ where $SI^{synovitis}$ is the average SI of the ROI set in the inflammatory synovial tissue, SI^{muscle} is the average SI of the ROI set in the normal muscle tissue and SD^{air} is the standard deviation of the SI of the air.

The same method was applied to measure on coronal fat-suppressed T2-weighted images the CNR of osteitis in abnormal medullary areas scored 3 by at least one reader whatever the MRI protocol. Defined ROIs between 10 and 60 mm^2 (mean 37.8 mm^2) in size were placed in the medullary areas scored 3, in medullary areas scored 0 and in the surrounding air on the coronal T2-weighted CHESS sequence and propagated on the corresponding coronal Dixon-based water-only images after synchronization. CNR was calculated with the following formula: $CNR^{osteitis} = 0.66 \times (SI^{osteitis} - SI^{bone\ marrow})/SD^{air}$ where $SI^{osteitis}$ is the average SI in the abnormal bone marrow, $SI^{bone\ marrow}$ the average SI in the normal bone marrow and SD^{air} the standard deviation of the SI the air.

2.4. Statistical analysis

Aggregated RAMRIS scores were calculated for synovitis ($RAMRIS^{synovitis}$), tenosynovitis ($RAMRIS^{tenosynovitis}$), osteitis ($RAMRIS^{osteitis}$) and erosions ($RAMRIS^{erosions}$) as the sum of the individual scores of both hands for synovitis, tenosynovitis, osteitis and erosions respectively. Total RAMRIS scores were calculated as the sum of the aggregated scores for synovitis, tenosynovitis, osteitis and erosions. If an individual score was declared not assessable on one MRI protocol, it was also considered non assessable on the other MRI protocol of the same patient.

Statistical analysis for the comparison of CNR consisted on a 2-way ANOVA test with fixed factors (fat suppression technique and type of measures) and 2-by-2 comparisons including paired *t*-test in case of normal distribution and Wilcoxon's signed ranks test in case of non-normal distribution. A p-value less than 0.05 was considered as statistically significant.

Inter-technique agreement, intra-observer agreement and inter-observer agreement were assessed using the paired differences in scores (the score obtained with the "Dixon-based protocol" minus the score obtained with the "CHESS-based protocol" for the inter-technique agreement, the score obtained by R1 at second reading minus the score obtained by R1 at first reading for the intra-observer agreement and the score obtained by R1 at first reading minus the score obtained by R2 at first reading for the inter-observer agreement) against the geometric mean of both scores according to the Bland and Altman methodology [17]. The mean bias and the limits of agreement were derived from each Bland-Altman plot. A paired *t*-test (normal distribution) or equivalently a non-parametric Wilcoxon rank-sum test (non-normal distribution) were performed to assess whether the median bias was significantly different from 0. The regression line of the differences was also computed and the p-value resulting from a 2-sided *t*-test based on the null hypothesis that the slope of the regression was equal to zero was calculated. A p-value less than 0.05 was considered as statistically significant for these tests.

3. Results

3.1. Patients

Thirty-two consecutive study participants suspected with early RA were imaged at MRI. Four were excluded because of incomplete MRI examinations (premature termination of the MRI examination in 3 participants and impossibility to inject contrast material in one). Complete MRI examinations were obtained in 28 study participants with motion artefacts observed and considered not to alter the analysis of the images in three participants.

Final diagnosis of the 28 included participants was ACPA-positive RA in 20 patients (71.4 %), ACPA-negative RA in five (17.9 %), undifferentiated arthritis in two (7.1 %) and monoarthritis in one participant (3.6 %). All study participants met the ACR/EULAR 2010 criteria for RA except one with ACPA-negative RA [18].

There was no statistically significant difference between the "2D SE T1" and "3D GRE T1" groups concerning sex (10 women / 4 men in the "2D SE T1" versus (vs.) 9 women / 5 men in the and "3D GRE T1" group; $p = 0.699$), age (46.1 years ± 14.6 vs. 44.4 years ± 15.0; $p = 0.791$), time between the suspicion of active RA by the rheumatologist and the MRI examination by the radiologist (22.4 days ± 22.1 vs. 22.6 days ± 39.4; $p = 0.981$), mean CRP blood level (27.1 $mg.L^{-1}$ ± 28.8 vs. 15.6 $mg.L^{-1}$ ± 20.4; $p = 0.811$) and DAS28-CRP (5.2 ± 1.1 vs. 4.7 ± 1.4; $p = 0.909$).

3.2. Comparison of fat suppression between Dixon- and CHESS-based MRI protocols

Among the series of 28 Dixon- and 28 CHESS-based MRI protocols, fat suppression failure was observed in 1 Dixon- and 25 CHESS-based

protocols by R1 and in 0 Dixon- and 23 CHESS-based protocols by R2.

On T2-weighted sequences, R1 observed fat suppression failure in 0.2 % of the areas to score with the Dixon images and 29.7 % of the areas to score on the CHESS images. On enhanced 2D SE T1-weighted sequences, R1 observed fat suppression failure in 0% of the areas to score with the Dixon images and 4.7 % of the areas to score with the CHESS images (Table 2) (Fig. 1).

Gradings of fat suppression effectiveness by R2 agreed with those of R1 in 91.3 % of the areas to score.

3.3. Comparison of CNRs between Dixon- and CHESS-based MRI protocols

$CNR^{synovitis}$ and $CNR^{osteitis}$ were measured in the synovial tissue of 43 joints (six study participants from the "2D SE T1" group and six from the "3D GRE T1" group) and in the medullary cavity of 35 bones (10 patients) (Table 3). $CNR^{synovitis}$ was statistically significantly higher on axial 2D SE ($p < 0.0001$) and 3D GRE ($p < 0.042$) contrast-enhanced T1-weighted Dixon water-only images than on corresponding CHESS images. $CNR^{osteitis}$ was statistically significantly lower on coronal T2-weighted Dixon water-only images than on corresponding CHESS images ($p < 0.0002$).

3.4. Comparison of RAMRIS scores between Dixon- and CHESS-based MRI protocols

RAMRIS scoring was feasible in all joints, tendons and bone except synovitis in 1/3 distal radioulnar joints for R1/R2 respectively. Mean aggregated and total RAMRIS scores of the "2D SE T1" group were not statistically significantly different from those of the "3D GRE T1" group ($p > 0.129$) (Table 4). Median bias and regression slopes of the differences between Dixon- and CHESS-based RAMRIS scores were not statistically significantly different from 0 for both readers in "2D SE T1" and "3D GRE T1" groups (Table 5) (Figs. 2–5).

3.5. Intra-observer reproducibility for RAMRIS scores on Dixon- and CHESS-based MRI protocols

In the "2D SE T1" group, differences between $RAMRIS^{synovitis}$, $RAMRIS^{tenosynovitis}$ and $RAMRIS^{erosions}$ at first and second readings were not statistically significantly different from 0 with the Dixon- and CHESS-based MRI protocols.

Table 2
Frequency of partial and complete fat suppression failure (FSF) in areas to score by the RAMRIS on fat-suppressed images of the Dixon- and CHESS-based MRI protocols for the two readers.

	Dixon-based MRI protocol			CHESS-based MRI protocol		
	2D SE T1	3D GRE T1	2D SE T2	2D SE T1	3D GRE T1	2D SE T2
R1						
Partial FSF	0/616	0/616	3/1400 (0.2 %)	19/616 (3.1 %)	0/616	221/1400 (15.8 %)
Complete FSF	0/616	0/616	0/1400	10/616 (1.6 %)	0/616	194/1400 (13.9 %)
R2						
Partial FSF	0/616	0/616	0/1400	8/616 (1.3 %)	0/616	160/1400 (11.4 %)
Complete FSF	0/616	0/616	0/1400	5/616 (0.8 %)	0/616	196/1400 (14.0 %)

N.B.: 616 joints and tendons were assessed for (teno)synovitis in 14 study participants on contrast-enhanced 2D SE T1-weighted images (8 joints and 14 tendons per hand) and 616 joints and tendons were assessed for (teno)synovitis in 14 study participants on contrast-enhanced 3D GRE T1-weighted images (8 joints and 14 tendons per hand); 1400 bones were assessed for osteitis in 28 study participants on T2-weighted images (25 bones per hand).

In the "3D GRE T1" group, differences between $RAMRIS^{tenosynovitis}$ at first and second readings were not statistically significantly different from 0 with the Dixon- and CHESS-based MRI protocols. Median bias of the differences between $RAMRIS^{synovitis}$ at first and second readings was statistically significantly different from 0 only with the CHESS-based MRI protocol (mean bias of +1.7; $p = 0.0305$). Regression slope of the differences between $RAMRIS^{erosions}$ at first and second readings was statistically significantly different from 0 only with the CHESS-based MRI protocol (+0.6; $p = 0.0039$).

In all study participants, regression slope of the differences between $RAMRIS^{osteitis}$ at first and second readings was statistically significantly different from 0 only with the CHESS-based MRI protocol (−0.8; $p = 0.0026$) (Table 5).

3.6. Inter-observer reproducibility for RAMRIS scores on Dixon- and CHESS-based MRI protocols

In the "2D SE T1" group, differences between R1 and R2 $RAMRIS^{synovitis}$, $RAMRIS^{tenosynovitis}$ and $RAMRIS^{erosions}$ were not statistically significantly different from 0 with the Dixon- and CHESS-based MRI protocols.

In the "3D GRE T1" group, differences between R1 and R2 $RAMRIS^{synovitis}$ were not statistically significantly different from 0 with the Dixon- and CHESS-based MRI protocols. Regression slope of the differences between R1 and R2 $RAMRIS^{tenosynovitis}$ was statistically significantly different from 0 only with the CHESS-based MRI protocol (+1.1; $p = 0.0072$). Regression slope of the differences between R1 and R2 $RAMRIS^{erosions}$ was statistically significantly different from 0 with the Dixon- (−0.6; $p = 0.0216$) and CHESS-based (−0.6; $p = 0.0179$) MRI protocols.

In all study participants, median bias and regression slopes of the differences between R1 and R2 $RAMRIS^{osteitis}$ were statistically significantly different from 0 with the Dixon- (−2.4; $p \leq 0.0342$) and CHESS-based (−3.1; $p < 0.0001$) MRI protocols (Table 5).

4. Discussion

First, the current study performed in patients with suspicion of early RA confirmed the robustness of the Dixon fat suppression as previously demonstrated in hands of healthy volunteers and RA patients based on semi-quantitative or qualitative analysis [11–13].

Second, we demonstrated higher CNRs for synovitis and tenosynovitis on contrast-enhanced 2D SE and 3D GRE T1-weighted Dixon water-only images than on the corresponding CHESS images. Previous studies demonstrated higher image quality with the Dixon method than with the CHESS technique by subjective visual image analysis [11] or by measuring signal-to-noise ratio (SNR) in hands of healthy volunteers [12,13]. To our knowledge, no previous study compared CNRs between contrast-enhanced T1-weighted Dixon and CHESS sequences in the musculoskeletal system. Of note, we demonstrated lower CNR for osteitis on T2-weighted Dixon water-only images than on CHESS images. This observation contradicts those of previous studies demonstrating higher image quality with the Dixon method than with the CHESS technique by subjective visual image analysis in the spine [19] or by measuring SNR in the brachial plexus [20,21] or CNR in the sacroiliac joints [22]. In our T2-weighted CHESS sequence, bandwidth was three time narrower than the bandwidth of the Dixon sequence while NEX was twice that of the Dixon sequence. It remains to be validated whether these parameter variations may account at least partially for the lower CNR on the T2-weighted Dixon sequence [23].

Third, we demonstrated that Dixon-based RAMRIS scoring was more reproducible than CHESS-based RAMRIS scoring. At intra-observer reproducibility, there was no statistically significant difference between RAMRIS scores at first and second readings with the Dixon sequences whereas significant differences were present with the CHESS-based protocols. At inter-observer reproducibility, the two statistically

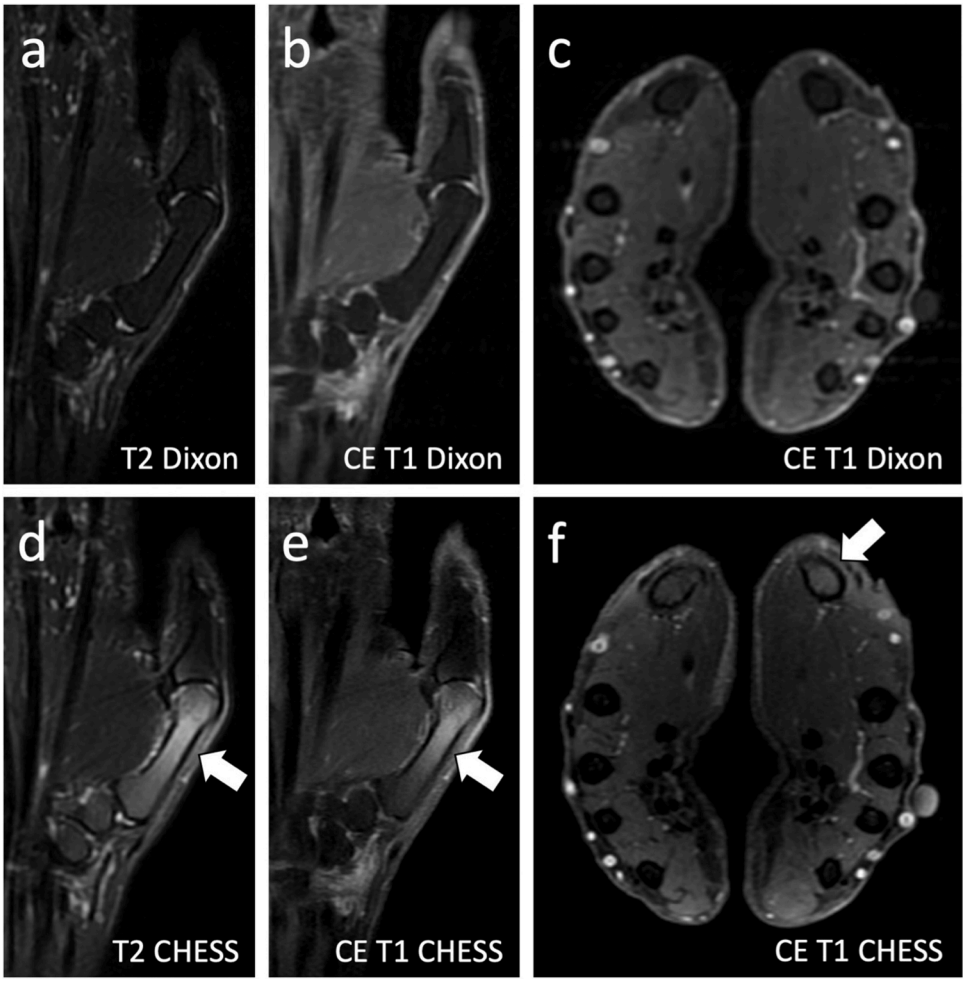

Fig. 1. Comparison between Dixon- (a–c) and CHESS-based (d–f) images of the right thumb of a 59-year-old RA patient. Fat suppression was effective on all Dixon images, including (a) T2-weighted Dixon water-only and contrast-enhanced 2D SE T1-weighted Dixon water-only images in the (b) coronal and (c) axial planes. Fat suppression failure occurred on all CHESS images (arrows) including (d) SE T2-weighted CHESS and contrast-enhanced 2D SE T1-weighted CHESS images in the (e) axial and (f) coronal planes.

Table 3
Comparison between CNRs (mean ± SD) for synovitis (contrast-enhanced fat-suppressed T1-weighted images) and osteitis (fat-suppressed T2-weighted images) on Dixon- and CHESS-based MRI protocols.

	Number of measures / Number of study participants	First sequences after contrast injection (Dixon / CHESS)	CNR Dixon (mean ± SD)	CNR CHESS (mean ± SD)	p
Synovitis 2D SE T1	32/6	16/16	110.0 ± 46.0	16.9 ± 10.9	<0.0001 *
Synovitis 3D GRE T1	11/6	5/6	389.8 ± 295.2	322.1 ± 239.9	0.042*
Osteitis 2D SE T2	35/10	–	43.2 ± 53.8	83.9 ± 46.3	0.0002*

* Statistically significantly different ($p < 0.05$).

significant differences occurring with Dixon sequences also occurred with the CHESS-based protocols.

Finally, we demonstrated that the Dixon-based RAMRIS scores were in agreement with the CHESS-based RAMRIS scores. These results make Dixon-based OMERACT-recommended MRI protocols a robust alternative to assess RAMRIS in early inflammatory arthritis at the cost of increased imaging time. Actually, the duration of the currently used Dixon-based MRI protocols was twice that of the CHESS-based OMERACT-recommended protocols. Our Dixon-based MRI protocols could

Table 4
Aggregated and total RAMRIS scores (mean ± SD) of "2D SE T1" and "3D GRE T1" groups with Dixon- and CHESS-based MRI protocols for R1 and R2.

	Reader 1−1st reading		Reader 1−2nd reading		Reader 2	
	Dixon	CHESS	Dixon	CHESS	Dixon	CHESS
RAMRIS scores in "2D SE T1" group (n = 14)						
Synovitis	13.0 ± 7.6	13.7 ± 8.1	13.5 ± 7.7	15.1 ± 7.1	13.8 ± 7.7	13.0 ± 7.4
Tenosynovitis	7.8 ± 5.9	6.8 ± 5.8	8.8 ± 6.2	7.4 ± 6.1	8.1 ± 6.5	6.7 ± 5.5
Osteitis	10.3 ± 16.1	10.6 ± 16.0	10.7 ± 14.6	9.1 ± 14.1	13.0 ± 18.3	15.2 ± 19.7
Erosions	4.3 ± 7.2	4.4 ± 6.6	4.4 ± 7.7	4.4 ± 6.6	4.8 ± 5.8	3.5 ± 6.0
Total	35.4 ± 30.4	35.6 ± 27.8	37.4 ± 29.9	35.9 ± 25.9	39.7 ± 31.3	38.4 ± 30.8
RAMRIS scores in "3D GRE T1" group (n = 14)						
Synovitis	8.6 ± 6.2	8.0 ± 5.4	9.4 ± 6.0	9.7 ± 6.6	8.3 ± 5.7	9.4 ± 5.3
Tenosynovitis	6.4 ± 4.6	7.1 ± 5.4	7.3 ± 4.1	8.4 ± 5.1	6.1 ± 3.6	6.1 ± 3.6
Osteitis	2.9 ± 4.2	2.9 ± 4.0	2.6 ± 3.6	2.9 ± 3.6	5.0 ± 4.5	4.6 ± 5.0
Erosions	0.4 ± 0.8	0.7 ± 1.1	0.4 ± 0.8	1.3 ± 1.8	1.0 ± 1.5	1.4 ± 1.9
Total	18.3 ± 11.5	18.8 ± 11.0	19.7 ± 10.9	22.4 ± 13.6	20.4 ± 10.2	21.4 ± 10.2

Table 5
Inter-technique agreement (Dixon-based RAMRIS – CHESS-based RAMRIS), intra-observer agreement (second reading RAMRIS – first reading RAMRIS) and inter-observer agreement (R1 RAMRIS – R2 RAMRIS) using Bland-Altman plots analysis with mean bias and limits of agreement.

		Synovitis		Tenosynovitis		Osteitis	Erosions	
		2D SE T1 (n = 14)	3D GRE T1 (n = 14)	2D SE T1 (n = 14)	3D GRE T1 (n = 14)	SE T2 (n = 28)	2D SE T1 (n = 14)	3D GRE T1 (n = 14)
Inter-technique agreement	R1 bias	−0.7 [-6.4;+5.0]	+0.6 [-4.9;+6.2]	+1.0 [-7.8;+9.8]	−0.8 [-5.6;+4.0]	−0.2 [-4.2;+3.8]	−0.1 [-3.6;+3.3]	−0.3 [-1.7;+1.1]
	R2 bias	+0.8 [-7.6;+9.2]	−1.1 [-6.8;+4.7]	+1.4 [-10.8;+13.6]	0.0 [-3.4;+3.4]	−0.9 [-10.7;+8.9]	+1.3 [-4.1;+6.6]	−0.4 [-3.6;+2.9]
Intra-observer agreement	Dixon bias	+0.5 [-3.5;+4.5]	+0.8 [-3.8;+5.3]	+1.0 [-4.3;+6.3]	+0.9 [-4.1;+6.0]	+0.1 [-4.5;+4.7]	+0.1 [-4.2;+4.5]	0.0 [-1.3;+1.3]
	CHESS bias	+1.4 [-5.0;+7.9]	+1.7* [-3.5;+6.9]	+0.6 [-2.8;+4.0]	+1.3 [-5.7;+8.3]	−0.8** [-6.8;+5.2]	−0.1 [-1.5;+1.4]	+0.6** [-1.4;+2.6]
Inter-observer agreement	Dixon bias	−0.8 [-11.4;+9.8]	+0.4 [-5.6;+6.3]	−0.4 [-8.0;+7.3]	+0.3 [-4.7;+5.2]	−2.4*/** [-11.9;+7.1]	−0.5 [-6.2;+5.2]	−0.6** [-3.6;+2.5]
	CHESS bias	+0.7 [-10.2;+11.7]	−1.4 [-8.8;+6.0]	+0.1 [-3.2;+3.4]	+1.1** [-5.5;+7.6]	−3.1*/** [-11.5;+5.2]	+0.9 [-4.5;+6.4]	−0.6** [-3.5;+2.2]

* Bias significantly different from 0 ($p < 0.05$).
** Regression slope significantly different from 0 ($p < 0.05$).

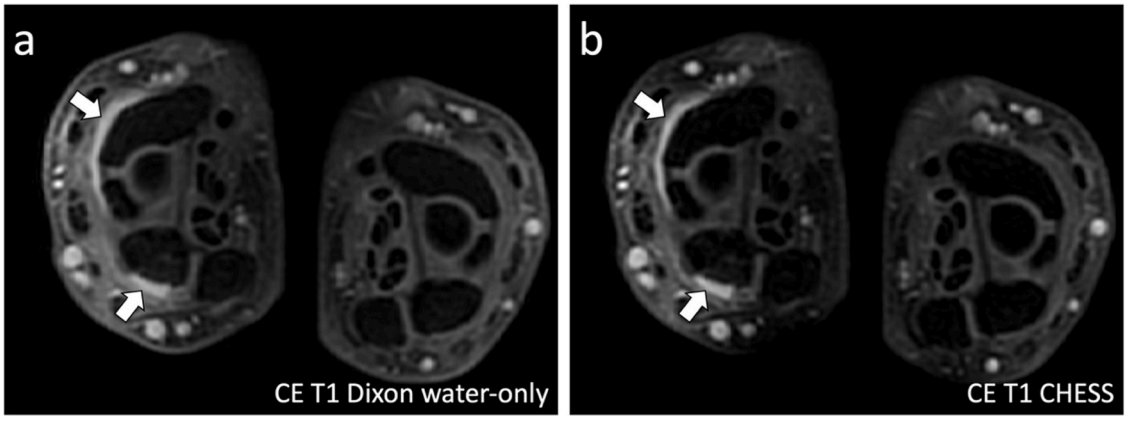

Fig. 2. Similar appearance of radio-carpal joint synovitis (white arrows) on axial contrast-enhanced 3D GRE T1-weighted (a) Dixon water-only and (b) CHESS images in a 30-year-old woman with early RA.

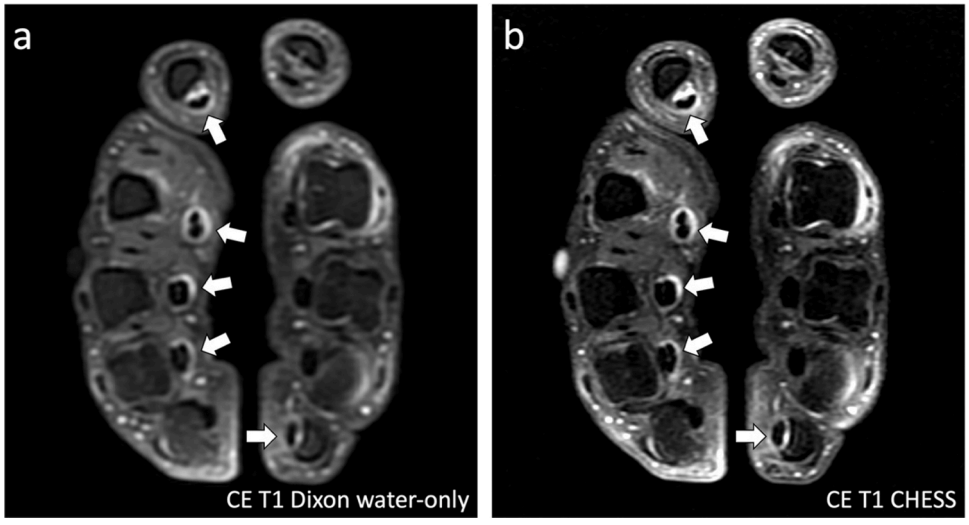

Fig. 3. Similar appearance of flexor pollicis longus and flexor digitorum tendons tenosynovitis (white arrows) on axial contrast-enhanced 2D SE T1-weighted (a) Dixon water-only and (b) CHESS images in a 28-year-woman with early RA.

have been more time-efficient and reduced by 4−5 min with the use of pre-contrast standard instead of Dixon T1-weighted sequences. We also acknowledge that the use of the 2-point instead of a 3-point Dixon method would have reduced the acquisition duration at the cost of a higher risk of fat-water swapping [7].

Our study has a few limitations. A major limitation of the current

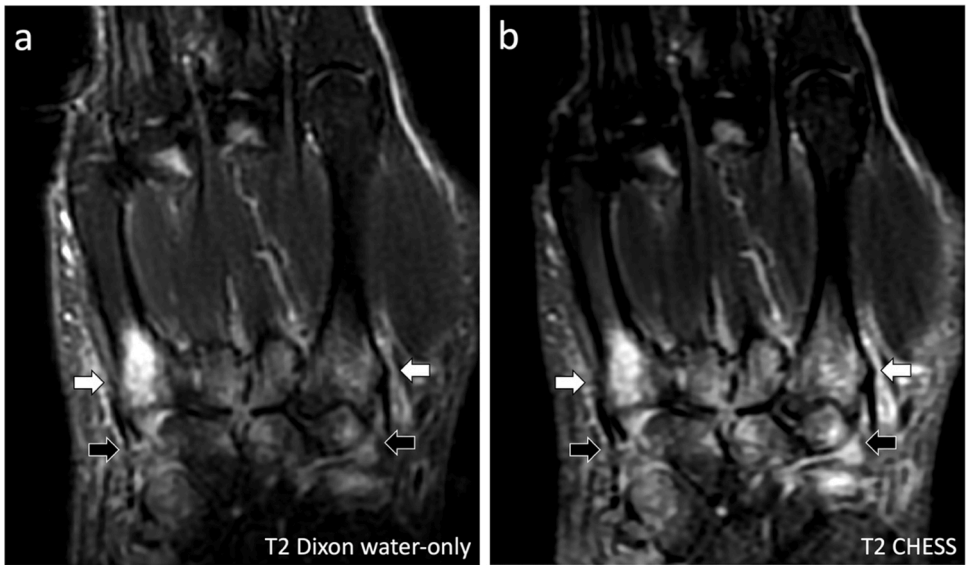

Fig. 4. Similar appearance of carpal (black arrows) and metacarpal (white arrows) bones osteitis on coronal SE T2-weighted (a) Dixon water-only and (b) CHESS focused images of a 56-year-old man with early RA.

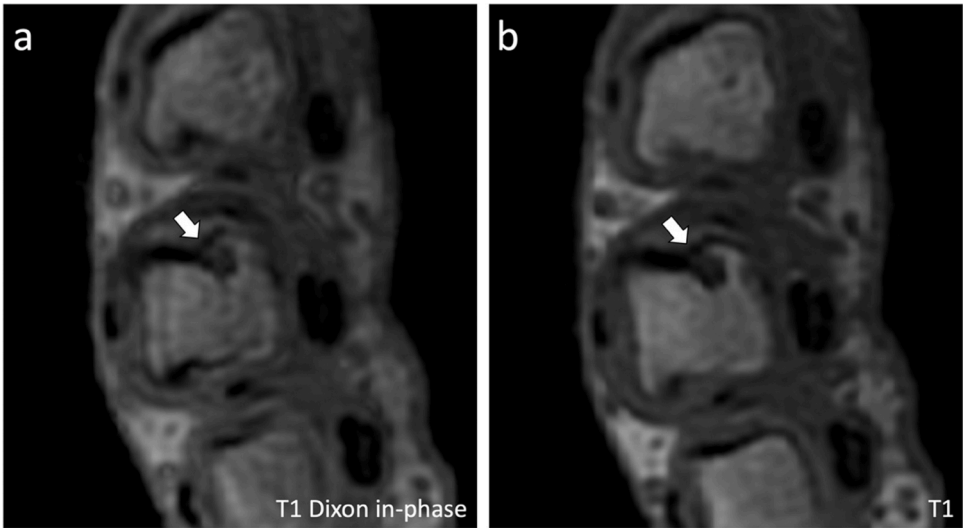

Fig. 5. Similar appearance of metacarpal head erosion (white arrows) on axial 3D GRE T1-weighted (a) Dixon in-phase and (b) non-Dixon focused images in a 60-year-old man with early RA.

study is its monocentric design with a limited number of patients and of readers. A multicentric study including more patients and more readers should be performed. Another limitation was the variability in the time delay between injection and sequence acquisition of the different MRI protocols. All contrast-enhanced sequences were obtained within 15 min after contrast-material injection ensuring optimal enhancement of inflammatory synovial tissue [24]. In our protocol, the acquisition order of the contrast-enhanced sequences (Dixon or CHESS sequences first) was alternated among study participants.

5. Conclusion

Three-point Dixon-based OMERACT-recommended MRI protocol at 1.5 T yields effective fat suppression, high T1-weighted image quality and reproducible assessment of disease activity in hands with early inflammatory arthritis.

Declaration of Competing Interest

The authors confirm that this work has not received any funding.

References

[1] M. Ostergaard, S. Møller-Bisgaard, Optimal use of MRI in clinical trials, clinical care and clinical registries of patients with rheumatoid arthritis, Clin. Exp. Rheumatol. 32 (Suppl. 85) (2014) S17–S22.
[2] M. Ostergaard, C. Peterfy, P. Conaghan, F. McQueen, P. Bird, B. Ejbjerg, R. Shnier, P. O'Connor, M. Klarlund, P. Emery, H. Genant, M. Lassere, J. Edmonds, OMERACT rheumatoid arthritis magnetic resonance imaging studies. Core set of MRI acquisitions, joint pathology definitions, and the OMERACT RA-MRI scoring system, J. Rheumatol. 30 (6) (2003) 1385–1386.
[3] M. Ostergaard, C.G. Peterfy, P. Bird, F. Gandjbakhch, D. Glinatsi, I. Eshed, E. A. Haavardsholm, S. Lillegraven, P. Boyesen, B. Ejbjerg, V. Foltz, P. Emery, H. K. Genant, P.G. Conaghan, The OMERACT rheumatoid arthritis magnetic resonance imaging (MRI) scoring system: updated recommendations by the OMERACT MRI in arthritis working group, J. Rheumatol. 44 (11) (2017) 1706–1712.
[4] I. Sudol-Szopinska, A.G. Jurik, I. Eshed, J. Lennart, A. Grainger, M. Ostergaard, A. Klauser, A. Cotten, M.C. Wick, M. Maas, F. Miese, N. Egund, N. Boutry,

M. Rupreht, M. Reijnierse, E.H. Oei, R. Meier, P. O'Connor, A. Feydy, V. Mascarenhas, A. Plagou, P. Simoni, H. Platzgummer, W.J. Rennie, A. Mester, J. Teh, P. Robinson, G. Guglielmi, G. Astrom, C. Schueller-Weiderkamm, Recommendations of the ESSR arthritis subcommittee for the use of magnetic resonance imaging in musculoskeletal rheumatic diseases, Semin. Musculoskelet. Radiol. 19 (4) (2015) 396–411.

[5] N. Boutry, M. Morel, R.M. Flipo, X. Demondion, A. Cotten, Early rheumatoid arthritis: a review of MRI and sonographic findings, AJR Am. J. Roentgenol. 189 (6) (2007) 1502–1509.

[6] D.A. Rubin, MRI and ultrasound of the hands and wrists in rheumatoid arthritis, I. Imaging findings, Skeletal Radiol 48 (5) (2019) 677–695.

[7] F. Del Grande, F. Santini, D.A. Herzka, M.R. Aro, C.W. Dean, G.E. Gold, J. A. Carrino, Fat-suppression techniques for 3-T MR imaging of the musculoskeletal system, Radiographics 34 (1) (2014) 217–233.

[8] Catherine Cyteval, Anne Miquel, Denis Hoa, Jean Pierre Daures, Xavier Mariette, Bernard Combe, Rheumatoid arthritis of the hand: monitoring with a simplified MR imaging scoring method— preliminary assessment, Radiology 256 (3) (2010) 863–869.

[9] N. Boutry, E. Hachulla, R.M. Flipo, B. Cortet, A. Cotten, MR imaging findings in hands in early rheumatoid arthritis: comparison with those in systemic lupus erythematosus and primary Sjogren syndrome, Radiology 236 (2) (2005) 593–600.

[10] H. Guerini, P. Omoumi, F. Guichoux, V. Vuillemin, G. Morvan, M. Zins, F. Thevenin, J.L. Drape, Fat suppression with Dixon techniques in musculoskeletal magnetic resonance imaging: a pictorial review, Semin. Musculoskelet. Radiol. 19 (4) (2015) 335–347.

[11] T. Aoki, Y. Yamashita, H. Oki, H. Takahashi, Y. Hayashida, K. Saito, Y. Tanaka, Y. Korogi, Iterative decomposition of water and fat with echo asymmetry and least-squares estimation (IDEAL) of the wrist and finger at 3T: comparison with chemical shift selective fat suppression images, J. Magn. Reson. Imaging 37 (3) (2013) 733–738.

[12] T. Kirchgesner, V. Perlepe, N. Michoux, A. Larbi, B. Vande Berg, Fat suppression at 2D MR imaging of the hands: Dixon method versus CHESS technique and STIR sequence, Eur. J. Radiol. 89 (2017) 40–46.

[13] T. Kirchgesner, V. Perlepe, N. Michoux, A. Larbi, B. Vande Berg, Fat suppression at three-dimensional T1-weighted MR imaging of the hands: Dixon method versus CHESS technique, Diagn. Interv. Imaging 99 (1) (2018) 23–28.

[14] T. Kirchgesner, B. Vande Berg, T. Sokolova, L. Meric de Bellefon, A. Nzeusseu, M. Stoenoiu, P. Durez, AB1352 evaluation of mri ramris score and clinical response in patients with acpa positive undifferentiated arthritistreated with infliximab versus placebo. Epidemiology, Risk Factors for Disease or Disease Progression, 2018, p. 1764, 2-1764.

[15] P. Bird, P. Conaghan, B. Ejbjerg, F. McQueen, M. Lassere, C. Peterfy, J. Edmonds, R. Shnier, P. O'Connor, E. Haavardsholm, P. Emery, H. Genant, M. Ostergaard, The development of the EULAR-OMERACT rheumatoid arthritis MRI reference image atlas, Ann. Rheum. Dis. 64 (Suppl 1) (2005) i8–10.

[16] H. Gudbjartsson, S. Patz, The Rician distribution of noisy MRI data, Magn. Reson. Med. 34 (6) (1995) 910–914.

[17] J.M. Bland, D.G. Altman, Measuring agreement in method comparison studies, Stat. Methods Med. Res. 8 (2) (1999) 135–160.

[18] D. Aletaha, T. Neogi, A.J. Silman, J. Funovits, D.T. Felson, C.O. Bingham 3rd, N. S. Birnbaum, G.R. Burmester, V.P. Bykerk, M.D. Cohen, B. Combe, K. H. Costenbader, M. Dougados, P. Emery, G. Ferraccioli, J.M. Hazes, K. Hobbs, T. W. Huizinga, A. Kavanaugh, J. Kay, T.K. Kvien, T. Laing, P. Mease, H.A. Menard, L. W. Moreland, R.L. Naden, T. Pincus, J.S. Smolen, E. Stanislawska-Biernat, D. Symmons, P.P. Tak, K.S. Upchurch, J. Vencovsky, F. Wolfe, G. Hawker, 2010 rheumatoid arthritis classification criteria: an American College of Rheumatology/ European League against Rheumatism collaborative initiative, Ann. Rheum. Dis. 69 (9) (2010) 1580–1588.

[19] J. Ma, S.K. Singh, A.J. Kumar, N.E. Leeds, J. Zhan, T2-weighted spine imaging with a fast three-point Dixon technique: comparison with chemical shift selective fat suppression, J. Magn. Reson. Imaging 20 (6) (2004) 1025–1029.

[20] S.B. Reeder, H. Yu, J.W. Johnson, A. Shimakawa, J.H. Brittain, N.J. Pelc, C. F. Beaulieu, G.E. Gold, T1- and T2-weighted fast spin-echo imaging of the brachial plexus and cervical spine with IDEAL water-fat separation, J. Magn. Reson. Imaging 24 (4) (2006) 825–832.

[21] A. Tagliafico, B. Bignotti, G. Tagliafico, C. Martinoli, Usefulness of IDEAL T2 imaging for homogeneous fat suppression and reducing susceptibility artefacts in brachial plexus MRI at 3.0 T, Radiol. Med. 121 (1) (2016) 45–53.

[22] A. Ozgen, The value of the T2-Weighted multipoint Dixon sequence in MRI of sacroiliac joints for the diagnosis of active and chronic sacroiliitis, AJR Am. J. Roentgenol. 208 (3) (2017) 603–608.

[23] D.G. Mitchell, S. Vinitski, M.D. Rifkin, D.L. Burk Jr., Sampling bandwidth and fat suppression: effects on long TR/TE MR imaging of the abdomen and pelvis at 1.5 T, AJR Am. J. Roentgenol. 153 (2) (1989) 419–425.

[24] N.F. Schwenzer, I. Kotter, J.C. Henes, C. Schraml, J. Fritz, C.D. Claussen, M. Horger, The role of dynamic contrast-enhanced MRI in the differential diagnosis of psoriatic and rheumatoid arthritis, AJR Am. J. Roentgenol. 194 (3) (2010) 715–720.